Mechanical Error Analysis of Disk Cam Mechanisms with a Flat-Faced Follower

Wen-Tung Chang*, Long-Iong Wu

Department of Power Mechanical Engineering, National Tsing Hua University, Hsinchu 30013, Taiwan

By employing the concept of equivalent linkage, this paper presents an analytical method for analyzing the mechanical errors of disk cam mechanisms with a flat-faced follower. The resulting error equations do not really involve the location of the curvature center of the cam profile, and locating the curvature center of the cam profile is not essential. The resulting errors are significantly affected by the pressure angle, and the smaller pressure angle will result in the smaller mechanical error. In the worst case, owing to the joined effects of various design parameters, the accuracy of the follower motion may degrade considerably. For the oscillating follower case, all acceleration error functions have a sudden change at every beginning and at every end of the motion even though the theoretical follower displacement is cycloidal motion.

Key Words: Disk Cam Mechanism, Mechanical Error Analysis, Equivalent Linkage, Tolerance, Flat-Faced Follower, Poppet Valve

Nomenclature

A : Contact point
A_n : Intersection of the contact normal of point A and the actual cam profile
A_r : Intersection of line O_2A and the actual cam profile
e : Follower offset
E : Point
f : Distance from the cam center to the follower pivot point
F : Constraint function of the equivalent linkage
I_{12}, I_{13}, I_{23} : Instant centers
K : Center of curvature of the cam profile
L : Theoretical displacement function of the translating follower $=L(\theta)$
O_2 : Fixed pivot of the cam
O_3 : Fixed pivot of the oscillating follower
P : Point
q : Distance from the cam center to the instant center I_{23}
Q : Location of the instant center I23
r : Radial dimension of the cam profile
r_1, r_2, r_4 : Link lengths
r_b : Radius of the base circle
S : Follower motion program $=S(\theta)$
t : Time
u : Distance from point P to point A
V : Follower velocity program $=V(\theta)$
V_Q : Speed of point Q
X_A, Y_A : X- and Y- components of the Cartesian coordinate of point A
α : Angle
Δ : Delta, variation
Δn : Normal-direction error of the cam profile
Δr : Radial direction error of the cam profile
ΔS : Follower motion error $=\Delta S(\theta)$
ΔS_e : ΔS due to Δe
ΔS_f : ΔS due to Δf
ΔS_{max} : Maximum value of ΔS
ΔS_n : ΔS due to Δn
ΔS_r : ΔS due to Δr

* Corresponding Author,
E-mail : wtchang@webmail.pme.nthu.edu.tw
TEL : +886-3-5715131 ext. 33755;
FAX : +886-3-5722840
Department of Power Mechanical Engineering, National Tsing Hua University, Hsinchu 30013, Taiwan.
(Manuscript **Received** August 26, 2005; **Revised** January 15, 2006)

ΔS_{rms} : Root-mean-square form of ΔS
ΔS_{wor} : Worst-case form of ΔS
ΔS_{ϕ} : ΔS due to $\Delta\phi$
θ : Cam rotation angle
θ_2, θ_3 : Angular displacements of links 2 and 3
λ : Shift angle, subtending angle of lines AA_n and AA_r
ξ : Theoretical angular displacement function of the oscillating follower $= \xi(\theta)$
ϕ : Pressure angle, oblique angle of the translating flat-faced follower
ω_2 : Angular velocity of the cam

1. Introduction

The cam mechanism provides a convenient and reliable means for motion control in machinery. In high-speed machinery, even small errors in cam contour may produce excessive noise, wear, and vibrations (Norton, 1988, 2002; Rothbart 2004). Therefore, for precision cam mechanisms, the follower motion has to be carefully controlled, and thus sufficient accuracy of the cam contour and consequent close tolerances are required to maintain reasonably acceptable performance of cam mechanisms. Because the tolerance applied to each dimension of the mechanism influences both function and cost, it is quite important to specify the tolerances at the largest (or optimal) values to meet the operating or functional considerations (Spotts, 1985). Consequently, the designer not only should know the effects of tolerances and clearances on the follower output functions, but also must decide about the levels of tolerances on various members of the mechanism for a specified maximum limit of the output mechanical error. That is, the mechanical error analysis (Hartenberg and Denavit, 1964; Grosjean, 1991) is the fundamental of optimal tolerance design for precision cam mechanisms.

There have been a variety of studies on the mechanical error analysis of disk cam mechanisms. Giordana et al.(1979), considering a cam mechanism from its equivalent four-bar linkage, dealt with the influence of construction and measurement errors on the motion deviation of the follower. Kim and Newcombe (1982) analyzed the effect of cam profile tolerance on the follower motion using the finite differences and the maximum likeihood method. Rao (1984) considered the tolerances of cam profile and other design parameters as random variables, and employed a stochastic approach for evaluating the actual kinematic response of the follower output. Chiu et al.(1993) applied the principle of the offset curve of a plane curve to perform the influence analysis of manufacturing and assembling errors of disk cam mechanisms. Wang et al.(1993) adopted the concept of normal-distributed profile tolerance and the Monte-Carlo method to simulate the machining error of the cam profile and the corresponding kinematic error of the follower. These approaches provided valuable source of ideas for this analysis, but they appear to have to deal with cumbersome equations and thus numerical evaluation of them involves much computation.

Wu and Chang (2005), employing the concept of equivalent linkage, proposed an analytical method for analyzing the mechanical errors of disk cams with a roller follower. However, most automobile engines use poppet valves, which are spring loaded closed and pushed open by overhead cams with a flat-faced follower attached to the valve stem (Pulkrabek, 1997). Compared with roller followers employed in engines, flat-faced followers could be simpler and more inexpensive. For this reason, it is necessary to further develop an analytical method for analyzing the mechanical errors of disk cams with a flat-faced follower.

2. Parametric Expressions for the Cam Profile

In order to find how the manufacturing error of a machined cam profile effects the corresponding output deviation of its follower, the analytical expressions for the theoretical cam profile should be derived first. The profile of a disk cam can be determined via the use of velocity instant centers (Davison, 1978; Rees-Jones, 1978a; Wu, 2003). For quick review and easy reference, the analytical approach for determining disk cam profiles parametrically in terms of the cam rotation angle

(Wu, 2003) is provided below. Here, disk cams with either an offset translating oblique flat-faced follower or an oscillating flat-faced follower are demonstrated.

2.1 Disk cam with an offset translating oblique flat-faced follower

Figure 1 shows a disk cam mechanism with an offset translating oblique flat-faced follower, which is a general form for actuating poppet valves of engines. Setting up a Cartesian coordinate system (X, Y) fixed on the cam and with its origin at the fixed pivot O_2, the cam profile coordinates may be expressed in terms of the cam rotation angle θ, which is measured against the direction of cam rotation from the reference radial to cam center parallel to follower translation. For simplicity, in the following, the ground link will be consistently numbered as 1, the cam as 2 and the follower as 3. By labeling instant center I_{23} as Q and $O_2Q=q$, the speed of point Q on the cam can be expressed as

$$V_Q=q\omega_2 \tag{1}$$

where ω_2 is the angular velocity of the cam and must be expressed in radians/sec. In order to let θ have a counterclockwise angle, in this paper, the cam is to rotate clockwise.

On the other hand, for a translating follower, all points on the follower have the same velocity.

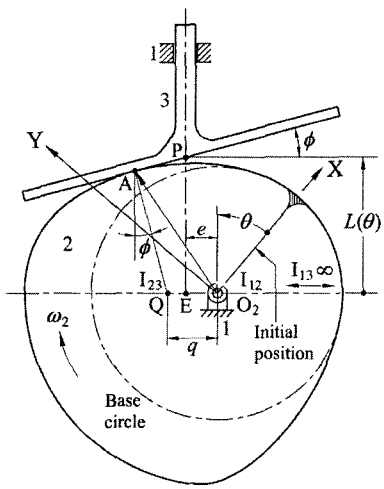

Fig. 1 Disk cam with an offset translating oblique flat-faced follower

Therefore, the speed of point Q on the follower can be expressed as

$$V_Q=\frac{dL(\theta)}{dt}=\frac{dL(\theta)}{d\theta}\frac{d\theta}{dt}=\frac{dL(\theta)}{d\theta}\omega_2 \tag{2}$$

where $L(\theta)$ is the displacement function of any reference point on the follower. If point P, the intersection of the follower surface and the ray passing through point E on the cam ($O_2E=e$) parallel to follower translation, is selected

$$L(\theta)=r_b\sec\phi-e\tan\phi+S(\theta) \tag{3}$$

Here, r_b is the radius of the base circle, ϕ is the oblique angle of the follower (i.e. the invariant pressure angle), e is the offset and $S(\theta)$ is the follower motion program. (The quantity ϕ is positive if the follower face is counterclockwise oblique from the horizontal; in the position shown it is positive. Also, since the cam is to rotate clockwise, the quantity e is negative if the offset is to the right; in the position shown it is positive.) Because instant center I_{23} (point Q) is a point common to links 2 (cam) and 3 (follower) having the same velocity, from Eqs. (1) and (2),

$$q=\frac{dL(\theta)}{d\theta}=\frac{dS(\theta)}{d\theta}=V(\theta) \tag{4}$$

where $V(\theta)$ is the follower velocity program. After r_b, ϕ, e and $S(\theta)$ have been selected, for each specified value of θ, the reference point P may be located by applying Eq. (3) and point Q by applying Eq. (4). From quadrangle EQAP,

$$QA=L(\theta)\cos\phi-(q-e)\sin\phi \tag{5}$$

Therefore, the vectors of the cam profile coordinates are

$$\mathbf{O_2A}=\mathbf{O_2Q}+\mathbf{QA} \tag{6}$$

where

$$\mathbf{O_2Q}=q\begin{Bmatrix}\cos(\theta+90°)\\ \sin(\theta+90°)\end{Bmatrix}=q\begin{Bmatrix}-\sin\theta\\ \cos\theta\end{Bmatrix} \tag{7}$$

$$\mathbf{QA}=QA\begin{Bmatrix}\cos(\theta+\phi)\\ \sin(\theta+\phi)\end{Bmatrix} \tag{8}$$

Hence, the parametric vector equations of the cam profile coordinates are

$$\mathbf{O_2A}=\begin{Bmatrix}X_A(\theta)\\ Y_A(\theta)\end{Bmatrix}=\begin{Bmatrix}QA\cos(\theta+\phi)-q\sin\theta\\ QA\sin(\theta+\phi)+q\cos\theta\end{Bmatrix} \tag{9}$$

For a translating flat-faced follower with zero oblique angle, $\phi=0°$, then

$$QA=L(\theta)=r_b+S(\theta) \tag{10}$$

That is, with zero oblique angle,the quantity e is not essential for determining the cam profile.

2.2 Disk cam with an oscillating flat-faced follower

Figure 2 shows a disk cam mechanism with an oscillating flat-faced follower. In this case, f represents the distance from the cam center to the follower pivot point and e represents the follower face offset from the follower pivot point. (If the follower face is offset from the pivot point towards the cam center, it is negative. The quantity e is positive in Fig. 2) Setting up a Cartesian coordinate system (X, Y) fixed on the cam and with its origin at the fixed pivot O_2, the cam profile coordinates may be expressed in terms of θ. The speed of point Q, instant center I_{23}, on the cam can be expressed as

$$V_Q=q\omega_2 \tag{11}$$

where $q=O_2Q$ and ω_2 is the angular velocity of the cam. On the other hand, the speed of point Q on the follower can be expressed as

$$V_Q=(f+q)\frac{d\xi(\theta)}{dt}=(f+q)\frac{d\xi(\theta)}{d\theta}\omega_2 \tag{12}$$

where $\xi(\theta)$ is the angular displacement function of the follower

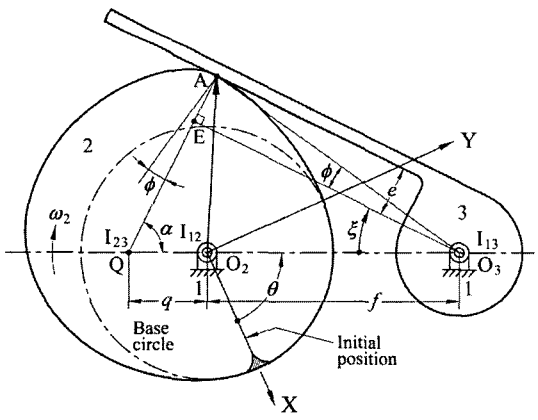

Fig. 2 Disk cam with an oscillating flat-faced follower

$$\xi(\theta)=\sin^{-1}\left(\frac{r_b-e}{f}\right)+S(\theta) \tag{13}$$

Here, r_b is the radius of the base circle, e is the offset of the follower and $S(\theta)$ is the follower angular motion program. From Eqs. (11) and (12) and after some algebraic manipulation,

$$q=\frac{f\dfrac{d\xi(\theta)}{d\theta}}{1-\dfrac{d\xi(\theta)}{d\theta}}=\frac{f\dfrac{dS(\theta)}{d\theta}}{1-\dfrac{dS(\theta)}{d\theta}}=\frac{fV(\theta)}{1-V(\theta)} \tag{14}$$

where $V(\theta)$ is the follower angular velocity program. From $\triangle O_3QE$,

$$QE=(f+q)\sin\xi(\theta) \tag{15}$$

$$\alpha=90°-\xi(\theta) \tag{16}$$

Therefore, the vectors of the cam profile coordinates are

$$\mathbf{O_2A}=\mathbf{O_2Q}+\mathbf{QA} \tag{17}$$

where

$$\mathbf{O_2Q}=q\begin{Bmatrix}\cos(\theta+180°)\\ \sin(\theta+180°)\end{Bmatrix}=q\begin{Bmatrix}\cos\theta\\ \sin\theta\end{Bmatrix} \tag{18}$$

$$\mathbf{OA}=(QE+e)\begin{Bmatrix}\cos(\theta+\alpha)\\ \sin(\theta+\alpha)\end{Bmatrix} \tag{19}$$

As a result, the parametric vector equations of the cam profile coordinates are

$$\mathbf{O_2A}=\begin{Bmatrix}X_A(\theta)\\ Y_A(\theta)\end{Bmatrix}=\begin{Bmatrix}(QE+e)\cos(\theta+\alpha)-q\cos\theta\\ (QE+e)\sin(\theta+\alpha)-q\sin\theta\end{Bmatrix} \tag{20}$$

From $\triangle O_3AE$, the pressure angle ϕ can be expressed as

$$\phi=\tan^{-1}\left[\frac{e}{(f+q)\cos\xi(\theta)}\right] \tag{21}$$

3. Equivalent Linkage and Mechanical Error Analysis

By employing the concept of equivalent linkage, the mechanical errors of disk cam mechanisms with a flat-faced follower can be determined analytically.

For the cam mechanism shown in Fig. 3(a), let point K be the center of curvature of the cam in contact with the follower (Rees-Jones, 1978b)

and point A be the contact point between cam and follower. Its equivalent linkage is the Scotch yoke mechanism shown in Fig. 3(b), in which the additional link is a floating slider block (link 4). The floating slider block pivots on one end of the crank (link 2) at the center of curvature of the cam, K, and connects the ground-connected slider (link 3) by a prismatic joint whose relative translation is along line AP. The characteristic length of the floating slider block r_4 is defined as KA in this paper. The instantaneous kinematic characteristics of the crank and the ground-connected slider are identical to those of the cam and the follower. Likewise, the cam mechanism with an oscillating flat-faced follower and its equivalent turning-block linkage (a slider-crank inversion) are shown in Figs. 4(a) and 4(b), respectively.

The actual profile of a machined cam may slightly deviate from the theoretical, and an error in the follower motion will thus be produced.

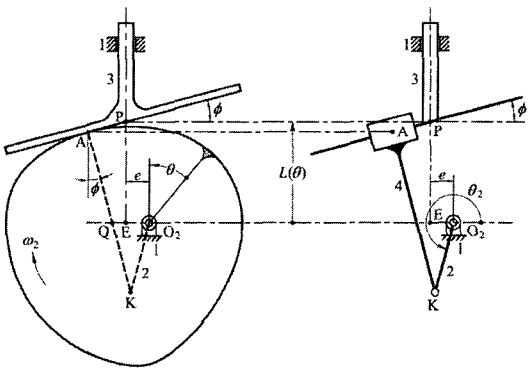

Fig. 3 A cam mechanism and its equivalent Scotch yoke mechanism

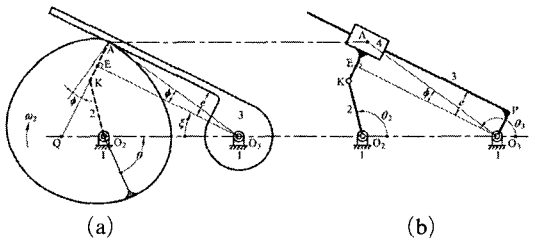

Fig. 4 A cam mechanism and its equivalent turning-block linkage

Since the instantaneous kinematic characteristics of a cam mechanism are identical to those of its equivalent linkage (Hall Jr., 1961 ; Hartenberg and Denavit, 1964), the mechanical error analysis of a cam mechanism can be performed through the aid of its equivalent linkage. In other words, if the profile error in the normal direction of a machined cam, Δn, equals the link-length error of the floating slider block, Δr_4, their output links will have the same motion deviations. As a result, the procedure developed by Hartenberg and Denavit (1964; Grosjean, 1991) can be applied to calculate the output motion deviation of the equivalent linkage.

3.1 Disk cam with an offset translating oblique flat-faced follower

For the equivalent linkage shown in Fig. 3(b), the displacement equation, relating the parameters ϕ, e, r_2, r_4 to the input and output variables θ_2 and $L(\theta)$, may be written as

$$F=r_2\sin(\theta_2-\phi)+r_4 -e\sin\phi-L\cos\phi=0 \tag{22}$$

where ϕ is the pressure angle, e is the offset, $r_2=O_2K$, and $r_4=KA$. For small values of the errors $\Delta\phi$, Δe, Δr_2, Δr_4, $\Delta\theta_2$ and ΔL, the differential of the function F may be written in terms of its partial derivatives as

$$dF\approx\Delta F=\frac{\partial F}{\partial\phi}\Delta\phi+\frac{\partial F}{\partial e}\Delta e+\frac{\partial F}{\partial r_2}\Delta r_2 +\frac{\partial F}{\partial r_4}\Delta r_4+\frac{\partial F}{\partial\theta_2}\Delta\theta_2+\frac{\partial F}{\partial L}\Delta L=0 \tag{23}$$

The output error ΔL is identical to the follower motion error ΔS. If the errors Δr_4, Δe and $\Delta\phi$ are independently considered to induce the output error ΔL, the mechanical errors at the output, ΔS_n due to Δn $(=\Delta r_4)$, ΔS_e due to Δe and ΔS_ϕ due to $\Delta\phi$, can be expressed as

$$\Delta S_n=\Delta L=-\frac{\partial F/\partial r_4}{\partial F/\partial L}\Delta r_4=\frac{\Delta r_4}{\cos\phi}=\frac{\Delta n}{\cos\phi} \tag{24}$$

$$\Delta S_e=\Delta L=-\frac{\partial F/\partial e}{\partial F/\partial L}\Delta e =-\frac{\sin\phi}{\cos\phi}\Delta e=-\Delta e\tan\phi \tag{25}$$

$$\Delta S_\phi=\Delta L=-\frac{\partial F/\partial\phi}{\partial F/\partial L}\Delta\phi$$
$$=\frac{L\sin\phi-e\cos\phi-r_2\cos(\theta_2-\phi)}{\cos\phi}\Delta\phi \quad (26)$$
$$=\frac{u}{\cos\phi}\Delta\phi$$

where

$$u=\mathrm{PA}=L\sin\phi+(q-e)\cos\phi \quad (27)$$

Here, u is the varying distance from the follower reference point P to the contact point A. (It should be noted that, in order to have consistent units, $\Delta\phi$ must be in radians. Then, a quantity with 'length' times 'angle in radian', such as ΔS_ϕ, may be regarded to have a dimension of 'length'.) For a translating flat-faced follower with zero oblique angle, $\phi=0°$ and Eq. (27) yields $u=\mathrm{PA}=(q-e)$, then Eqs. (24) ~ (26) yield

$$\Delta S_n=\Delta n \quad (28)$$

$$\Delta S_e=0 \quad (29)$$

$$\Delta S_\phi=(q-e)\Delta\phi \quad (30)$$

Equations (24) ~ (26) indicate that, as expected, the pressure angle have a significant effect on the resulting errors; it appears in the form of $(1/\cos\phi)$ to magnify them (Hartenberg and Denavit, 1964). In addition, it is interesting to note that in the final expressions of Eqs. (24) ~ (26), the parameters r_2 and r_4 are not actually involved. In other words, locating the curvature center of the cam profile in the analysis process is not really essential, and this fact makes the analysis easier to perform.

3.2 Disk cam with an oscillating flat-faced follower

For the equivalent linkage shown in Fig. 4(b), the displacement equation, relating the parameters e, r_1, r_2, r_4 to the input and output variables θ_2 and θ_3, may be written as

$$F=r_1\sin\theta_3+r_2\sin(\theta_2-\theta_3)-r_4+e=0 \quad (31)$$

where e is the follower offset, $r_1=\mathrm{O_2O_3}=f$, $r_2=\mathrm{O_2K}$, and $r_4=\mathrm{KA}$. For small values of the errors Δe, Δr_1, Δr_2, Δr_4, $\Delta\theta_2$ and $\Delta\theta_3$, the differential of the function F may be written in terms of its partial derivatives as

$$dF\approx\Delta F=\frac{\partial F}{\partial e}\Delta e+\frac{\partial F}{\partial r_1}\Delta r_1+\frac{\partial F}{\partial r_2}\Delta r_2$$
$$+\frac{\partial F}{\partial r_4}\Delta r_4+\frac{\partial F}{\partial\theta_2}\Delta\theta_2+\frac{\partial F}{\partial\theta_3}\Delta\theta_3=0 \quad (32)$$

Recall from Fig. 4 that $\xi(\theta)=180°-\theta_3$, and thus $\Delta S=\Delta\xi=-\Delta\theta_3$. If the errors Δr_4, Δr_1 and Δe are independently considered to induce the output error $\Delta\theta_3$, the mechanical errors at the output, ΔS_n due to Δn $(=\Delta r_4)$, ΔS_f due to Δf $(=\Delta r_1)$ and ΔS_e due to Δe, can be expressed as

$$\Delta S_n=-\Delta\theta_3=\frac{\partial F/\partial r_4}{\partial F/\partial\theta_3}\Delta r_4$$
$$=\frac{-\Delta r_4}{r_1\cos\theta_3-r_2\cos(\theta_2-\theta_3)} \quad (33)$$
$$=\frac{\Delta n}{u}=\frac{\Delta n\tan\phi}{e}$$

$$\Delta S_f=-\Delta\theta_3=\frac{\partial F/\partial r_1}{\partial F/\partial\theta_3}\Delta r_1$$
$$=\frac{\sin\theta_3}{r_1\cos\theta_3-r_2\cos(\theta_2-\theta_3)}\Delta r_1 \quad (34)$$
$$=-\frac{\Delta f\sin\xi}{u}=-\frac{\Delta f\sin\xi\tan\phi}{e}$$

$$\Delta S_e=-\Delta\theta_3=\frac{\partial F/\partial e}{\partial F/\partial\theta_3}\Delta e$$
$$=-\frac{\Delta e}{r_1\cos\theta_3-r_2\cos(\theta_2-\theta_3)} \quad (35)$$
$$=-\frac{\Delta e}{u}=-\frac{\Delta e\tan\phi}{e}$$

where

$$u=\mathrm{PA}=\mathrm{O_3E}=\frac{e}{\tan\phi}=(f+q)\cos\xi \quad (36)$$

Here, u is the varying distance from the follower reference point P, as shown in Fig. 4(b), to the contact point A. Equations (33) ~ (35) indicate that the pressure angle appears in the form of $\tan\phi$ to magnify the resulting errors. Also, in the final expressions of Eqs. (33) ~ (35), the parameters r_2 and r_4 are not actually involved, and thus locating the curvature center of the cam profile is not really essential.

3.3 Radial profile error and normal-direction error

In practice, the accuracy of a machined cam may be controlled through a properly specified tolerance of the radial dimension of the actual cam profile. In other words, the radial dimensions of the actual cam profile with corresponding cam angles must lie within a specified zone along the ideal profile. In order to find how the radial-dimension error of the actual cam profile affects the motion deviation of the follower, the correlation between the radial-dimension error and the normal-direction error of the cam profile must be established.

Figure 5 shows a cam in contact with its flat-faced follower, in which the theoretical cam profile is shown in full line and the actual cam profile in dashed line, and the profile deviation is exaggerated for clarity. The theoretical contact point is designated by A, and its normal to the cam profile intersects the actual cam profile at point A_n; line O_2A intersects the actual cam profile at point A_r. For a sufficiently small value of normal-direction profile error AA_n, since A_n A_r will be tangent to the actual cam profile and AnA will be normal to the profile, $\triangle AA_nA_r$ can be considered as a right-angled triangle, and thus

$$\Delta n \approx \Delta r \cos \lambda \tag{37}$$

where $\Delta n = AA_n$, $\Delta r = AA_r$ and $\lambda = \angle A_rAA_n$.

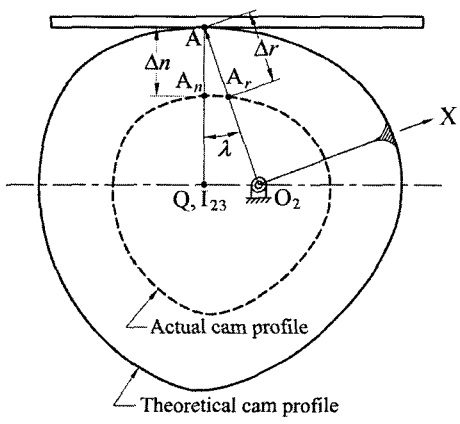

Fig. 5 Actual cam profile and theoretical cam profile

In addition, the common normal at the contact point A must always pass through point Q, which is also the instant center I_{23}, and so

$$\lambda = \angle O_2AQ \tag{38}$$

From $\triangle O_2AQ$,

$$\lambda = \sin^{-1}\left(\frac{\mathbf{QA} \times \mathbf{O_2A}}{\|\mathbf{QA}\| \cdot \|\mathbf{O_2A}\|}\right) \tag{39}$$

This is a general expression for the shift angle λ and is applicable to all types of disk cam mechanisms.

For the cam mechanism with an translating oblique flat-faced follower shown in Fig. 6(a), applying the sine law to $\triangle O_2AQ$ yields

$$\begin{aligned}\lambda &= \sin^{-1}\left[\frac{q \sin(\phi + 90°)}{\|\mathbf{O_2A}\|}\right] \\ &= \sin^{-1}\left[\frac{V(\theta)\cos\phi}{\|\mathbf{O_2A}\|}\right]\end{aligned} \tag{40}$$

where $\angle O_2QA = \phi + 90°$. From Eqs. (24), (37) and (40), the final result is

$$\Delta S_r = \Delta L \approx \frac{\Delta r \cos \lambda}{\cos \phi} \tag{41}$$

This shows how the radial-dimension error of the cam profile affects the motion deviation of the translating follower. Note that the follower motion deviation ΔS_r is dominated by the shift angle λ with the form of $\cos \lambda$, since the pressure angle ϕ is a constant.

Similarly, for the cam mechanism with an oscillating flat-faced follower shown in Fig. 6(b), applying the sine law to $\triangle O_2AQ$ yields

$$\begin{aligned}\lambda &= \sin^{-1}\left(\frac{q \sin \alpha}{\|\mathbf{O_2A}\|}\right) \\ &= \sin^{-1}\left\{\frac{fV(\theta)\cos\xi(\theta)}{[1 - V(\theta)]\|\mathbf{O_2A}\|}\right\}\end{aligned} \tag{42}$$

where α is defined in Eq. (16). From Eqs. (33), (37) and (42), the final result is

$$\Delta S_r = -\Delta\theta_3 \approx \frac{\Delta r \cos \lambda}{u} = \frac{\Delta r \cos \lambda \tan \phi}{e} \tag{43}$$

This shows how the radial-dimension error of the cam profile affects the motion deviation of the oscillating follower. In this case, the effect

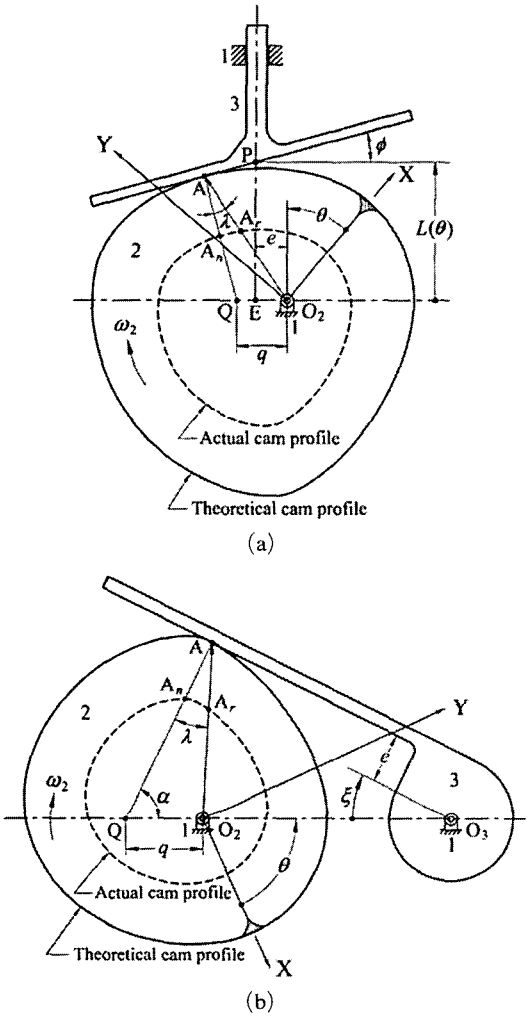

Fig. 6 Disk cam mechanisms and their actual cam profiles

of the pressure angle (in the form of $\tan\phi$) is multiplied by the shift angle (in the form of $\cos\lambda$).

3.4 Velocity and acceleration errors

Since the equivalent linkage method provides the closed-form solutions for the displacement error functions of the follower, its corresponding velocity and acceleration error functions can also be expressed analytically. The velocity and acceleration error analysis is straightforwardly performed by differentiating the obtained displacement error functions with respect to time once and twice. The analytical expressions are tedious and not shown here, while numerical solutions are suggested instead.

4. Examples

The method presented above will be illustrated by the following examples.

Example 1: A cam system requires the offset translating oblique flat-faced follower to rise 22 mm with cycloidal motion while the cam rotates clockwise from 0° to 120°, dwell for the next 70°, return with cycloidal motion for 100° cam rotation and dwell for the remaining . The offset, e, is 10 mm ; the oblique angle, ϕ, is 15°. The radius of the base circle, r_b, is 40 mm.

The cam profile, which has a maximum radial dimension of 61.25 mm, is shown in Fig. 1. For a tolerance grade of IT6, the cam profile may have a deviation of $\Delta r=19\ \mu$m, the offset may have a deviation of $\Delta e=9\ \mu$m, and the oblique angle may have a deviation of $\Delta\phi=0.011°=1.92\times10^{-4}$ rad. The motion of the follower will then have deviations result from them, ΔS_r due to Δr, ΔS_e due to Δe and ΔS_ϕ due to $\Delta\phi$, respectively. The worst-case deviation of the follower motion will be

$$\Delta S_{wor}=|\Delta S_r|+|\Delta S_e|+|\Delta S_\phi| \tag{44}$$

The maximum expected deviation of the follower motion will be (Garrett and Hall Jr., 1969)

$$\Delta S_{rms}=\sqrt{\Delta S_r^2+\Delta S_e^2+\Delta S_\phi^2} \tag{45}$$

which is often referred to as the root mean square value (Hartenberg and Denavit, 1964 ; Grosjean, 1991).

All functions that might be of interest are shown in Fig. 7, and their extreme values are also listed in Table 1. Figure 7(a) shows that the shift angle λ, having quiet similar trend to the varying distance u, is zero at the two dwell regions ($\theta=120°\sim190°$ and $\theta=290°\sim360°$). However, the shift angle λ, which appears in the form of $\cos\lambda$, is more non-sensitive than the varying distance u in essence to magnify the resulting errors. In Fig. 7(b), one non-dimensional factor ($u/u_{max}\cos\phi$) rather than ($u/\cos\phi$) is given to compare

with the other non-dimensional factor ($\cos\lambda/\cos\phi$). As seen, since $0.9297 \leq (\cos\lambda/\cos\phi) \leq 1.0353$, its magnitude has only slight variation. Hence, the variation of ΔS_r is flatter than that of ΔS_ϕ, as shown in Fig. 7(c). Since the variation of ΔS_r is dominated by $(\cos\lambda/\cos\phi)$, it has an extreme value of 19.67 μm at the two dwell regions. In addition, owing to that $\tan\phi=0.2679$ is a constant, the magnitude of $\Delta S_e=-2.41$ μm is invariant.

Table 1 Input angles and extreme values (example 1)

Input angle	Extreme value
$\theta=54.84°$	$\lambda_{max}=22.21°$
$\theta=63.41°$	$u_{max}=23.67$ mm
$\theta=63.41°$	$(\Delta S_\phi)_{max}=4.704$ μm
$\theta=71.5°$	$(\Delta S_{wor})_{max}=25.57$ μm
$\theta=103.89°$	$(\Delta S_{rms})_{max}=19.87$ μm
$\theta=120°\sim190°$	$(\cos\lambda/\cos\phi)_{max}=1.0353$
$\theta=120°\sim190°$	$(\Delta S_r)_{max}=19.67$ μm
$\theta=206.39°$	$(\Delta S_{wor})_{min}=21.99$ μm
$\theta=242.37°$	$u_{min}=-21.27$ μm
$\theta=242.37°$	$(\Delta S_\phi)_{max}=-4.23$ μm
$\theta=244.31°$	$(\cos\lambda/\cos\phi)_{min}=0.9297$
$\theta=244.31°$	$\lambda_{min}=-26.1°$
$\theta=244.31°$	$(\Delta S_r)_{min}=17.66$ μm
$\theta=245.23°$	$(\Delta S_{rms})_{max}=18.32$ μm
$\theta=290°\sim360°$	$(\cos\lambda/\cos\phi)_{max}=1.0353$
$\theta=290°\sim360°$	$(\Delta S_r)_{max}=19.67$ μm

The extreme value of ΔS_{wor} occurring at $\theta=71.5°$ is 25.57 μm. From the viewpoint of the position accuracy of the follower motion, for a total follower travel of 22 mm, a position deviation of $\Delta S_{max}=25.57$ μm implies a lower accuracy. That is, if the worst situation occurs, the follower motion will have a degraded accuracy of IT7 (21 μm) ~IT8 (33 μm).

The velocity error functions ΔV_r due to Δr, ΔV_e due to Δe and ΔV_ϕ due to $\Delta\phi$ are shown in Fig. 8(a). The acceleration error functions ΔA_r due to Δr, ΔA_e due to Δe and ΔA_ϕ due to $\Delta\phi$ are shown in Fig. 8(b). As a result of that ΔS_e is invariant, the corresponding ΔV_e and ΔA_e are both zero. Note that in the acceleration error functions, there is a sudden change at every beginning and at every end of ΔA_ϕ,

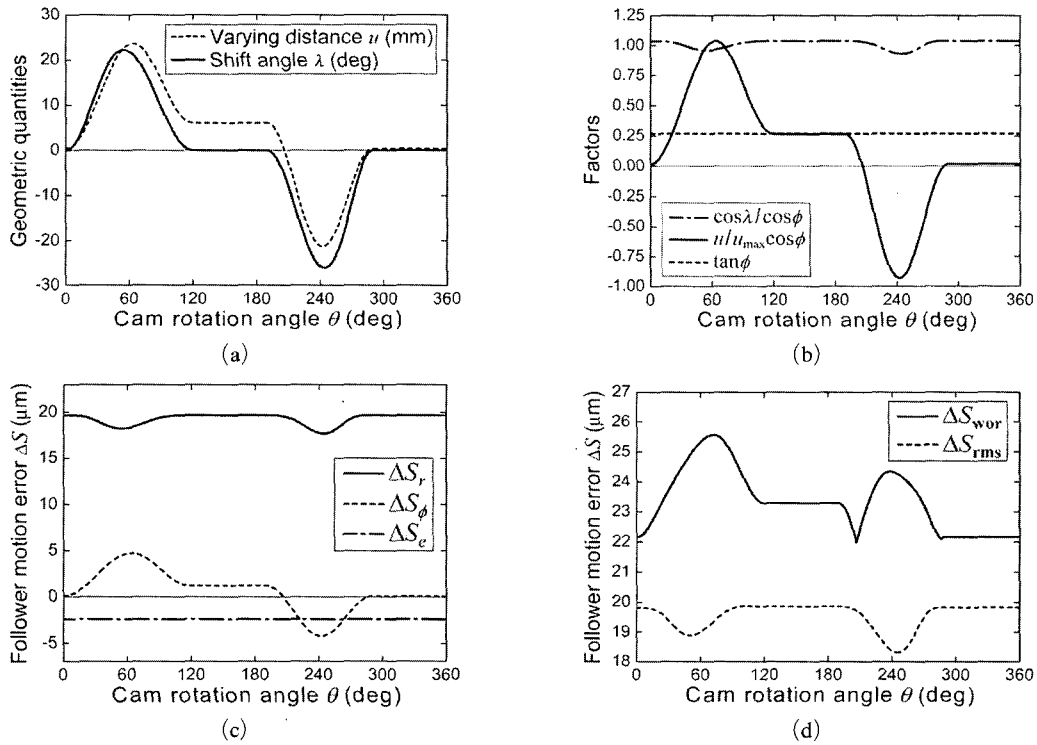

Fig. 7 Mechanical error analysis of a cam mechanism (example 1)

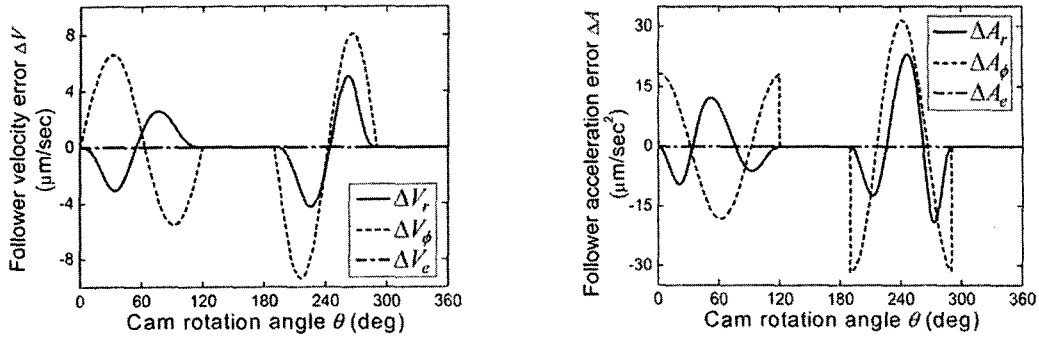

(a) (b)

Fig. 8 Velocity and acceleration error functions of a cam mechanism (example 1)

although the theoretical follower displacement is cycloidal motion. On the contrary, ΔA_r is a continuous and smooth function, since cos λ may have continuous derivatives to the second order at least.

Example 2: A cam system requires the oscillating flat-faced follower to oscillate 15° clockwise with cycloidal motion while the cam rotates clockwise from 0° to 120°, dwell for the next 40°, return with cycloidal motion for 120° cam rotation and dwell for the remaining 80°. The distance between pivots, f, is 80 mm ; the offset of the follower face, e, is 16 mm. The base circle radius, r_b, is 40 mm.

The cam profile, which has a maximum radial dimension of 58.934 mm, is shown in Fig. 2. For a tolerance grade of IT6, the cam profile and the distance between pivots may have the same deviation of $\Delta r=\Delta f=19$ μm, and the offset may have a deviation of $\Delta e=11$ μm. Then the motion of the follower will have deviations result from them, ΔS_r due to Δr, ΔS_f due to Δf, and ΔS_e due to Δe, respectively. The worst-case deviation of the follower motion will be

$$\Delta S_{wor}=|\Delta S_r|+|\Delta S_f|+|\Delta S_e| \tag{46}$$

The maximum expected deviation of the follower motion will be (Garrett and Hall Jr., 1969)

$$\Delta S_{rms}=\sqrt{\Delta S_r^2+\Delta S_f^2+\Delta S_e^2} \tag{47}$$

which is often referred to as the root mean square value (Hartenberg and Denavit, 1964 ; Grosjean, 1991).

Table 2 Input angles and extreme values (example 2)

Input angle	Extreme value
$\theta=31.18°$	$(\Delta S_f)_{max}=-0.0041°$
$\theta=52.42°$	$(\Delta S_{wor})_{min}=0.021°$
$\theta=53.92°$	$(\Delta S_{rms})_{min}=0.0128°$
$\theta=55.4°$	$\lambda_{max}=26.355°$
$\theta=55.61°$	$(\cos\lambda\tan\phi)_{min}=0.1476$
$\theta=55.61°$	$(\Delta S_r)_{min}=0.01°$
$\theta=55.77°$	$\phi_{min}=9.355°$
$\theta=55.77°$	$(\tan\phi)_{min}=0.1647$
$\theta=55.77°$	$(\Delta S_e)_{max}=-0.0065°$
$\theta=192.72°$	$(\Delta S_f)_{min}=-0.0092°$
$\theta=203.54°$	$(\Delta S_{wor})_{max}=0.0382°$
$\theta=204.96°$	$(\Delta S_{rms})_{max}=0.0231°$
$\theta=207.4°$	$(\cos\lambda\tan\phi)_{max}=0.2695$
$\theta=207.4°$	$(\Delta S_r)_{max}=0.0183°$
$\theta=212.11°$	$\phi_{max}=15.535°$
$\theta=212.11°$	$(\tan\phi)_{max}=0.278$
$\theta=212.11°$	$(\Delta S_e)_{min}=-0.0109°$
$\theta=227.43°$	$\lambda_{min}=-16.751°$

All functions that might be of interest are shown in Fig. 9, and their extreme values are also listed in Table 2. Figure 9(a) shows that the range of the pressure angle is $9.355°\leq\phi\leq15.535°$; its variation is much slighter than that of the shift angle λ ($-16.751°\leq\lambda\leq26.355°$). Hence, the factors ($\cos\lambda\tan\phi$) and $\tan\phi$ shown in Fig. 9 (b) have quiet similar trend. This situation results in that the occurrence of extreme values of ΔS_r (occurring at $\theta=55.61°$ and $\theta=207.4°$) are close to those of ΔS_e (occurring at $\theta=55.77°$ and $\theta=212.11°$).

The extreme value of ΔS_{wor} occurs at $\theta=$

203.54°, close to θ=212.11° where the extreme pressure angle ϕ occurs. The worst-case deviation has an extreme magnitude of ΔS_{max}=0.0382°. From the viewpoint of the position accuracy of the follower motion, for a total follower travel of 15°, an angular position deviation of ΔS_{max}= 0.0382° implies a quite low accuracy. In other words, if the worst situation occurs, the follower motion will have a degraded accuracy of IT8 (0.027°) ~IT9 (0.043°).

The velocity error functions ΔV_r due to Δr, ΔV_e due to Δe and ΔV_f due to Δf are shown in Fig. 10(a). Their corresponding acceleration error functions are shown in Fig. 10(b). In this case, they all have a sudden change at every beginning and at every end of the motion, although the theoretical follower displacement is cycloidal motion.

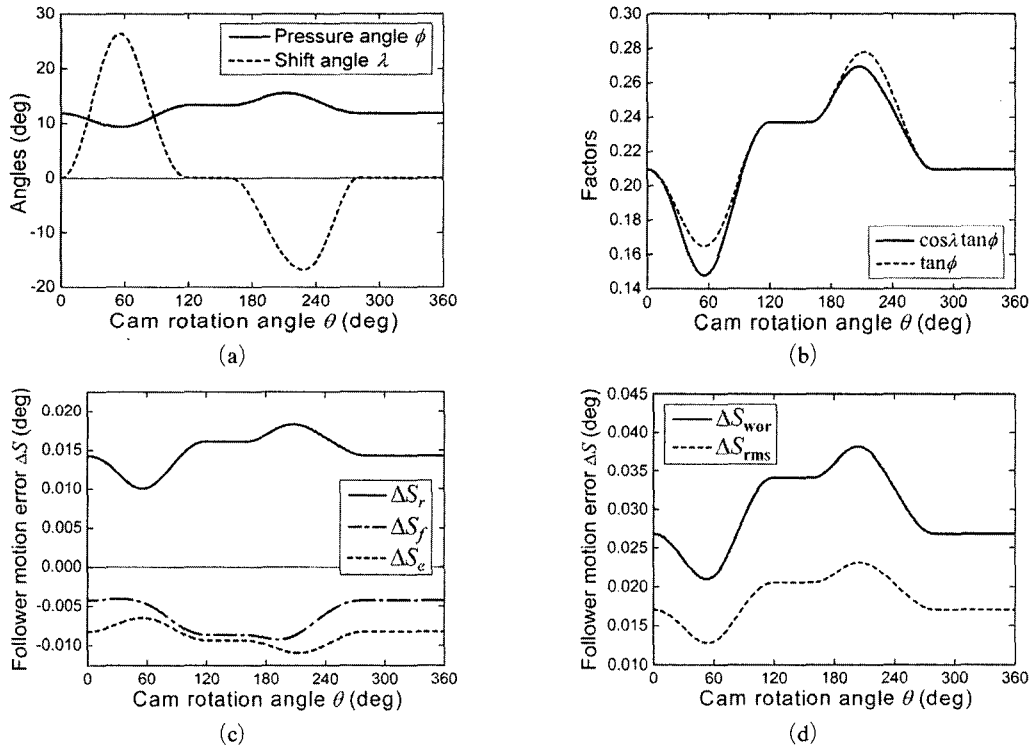

Fig. 9 Mechanical error analysis of another cam mechanism (example 2)

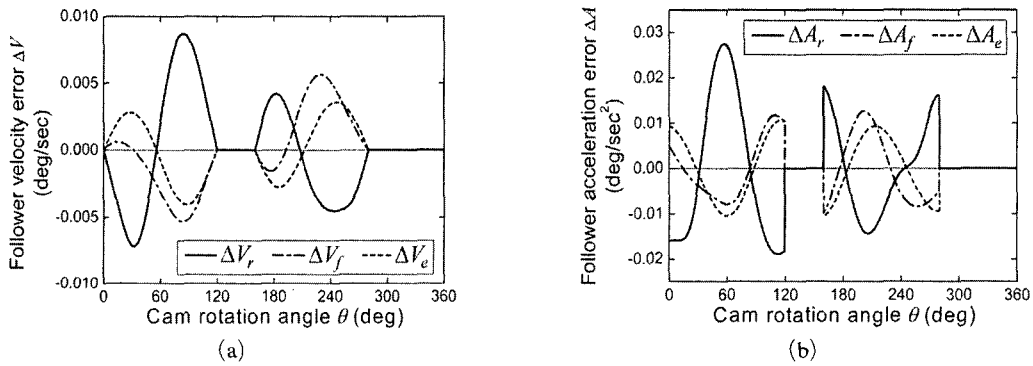

Fig. 10 Velocity and acceleration error functions of another cam mechanism (example 2)

5. Conclusions

By employing the concept of equivalent linkage, the mechanical errors of disk cams with a flat-faced follower can be determined analytically. The resulting error equations do not really involve the location of the curvature center of the cam profile, and thus locating the curvature center of the cam profile is not essential. For the flat-faced follower cases, the resulting errors are also significantly affected by the pressure angle, and the smaller pressure angle will result in the smaller mechanical error. The design parameter that may result in a larger resulting error should have a smaller tolerance. In the worst case, owing to the joined effects of various design parameters, the accuracy of the follower motion may degrade considerably. For the oscillating follower case, all acceleration error functions have a sudden change at every beginning and at every end of the motion even though the theoretical follower displacement is cycloidal motion. However, for the translating follower case, neither the error of the cam profile nor the variation of offset amount will cause sudden change of the acceleration error function. This implies that a translating flat-faced follower is a potentially superior choice to an oscillating flat-faced follower for actuating poppet valves of engines. The presented method for mechanical error analysis of disk cam mechanisms and the obtained results may be helpful for tolerance specification in cam design.

Acknowledgments

The authors are grateful to the National Science Council of the Republic of China for supporting this research under grant NSC 94-2212-E-007-030.

References

Chiu, H., Ozaki, H., Sato, E., Suzuki, T., Oho, A. and Ariura, Y., 1993, "An Analysis Using Offset Curves for Profiles, Manufacturing and Errors of Plane Cams." *JSME International Journal-Part C*, Vol. 36, No. 1, pp. 110~118.

Davison, J. K., 1978, "Calculating Cam Profiles Quickly," *Machine Design*, 7 December, pp. 151~155.

Garrett, R. E. and Hall Jr., A. S., 1969, "Effect of Tolerance and Clearance in Linkage Design," *ASME Journal of Engineering for Industry*, Vol. 91B, pp. 198~202.

Giordana, F., Rognoni, V. and Ruggieri, G., 1979, "On the Influence of Measurement Errors in the Kinematic Analysis of Cams," *Mechanism and Machine Theory*, Vol. 14, No. 5, pp. 327~340.

Grosjean, J., 1991, *Kinematics and Dynamics of Mechanisms*, McGraw-Hill, New York, pp. 267~285.

Hall Jr., A. S., 1961, *Kinematics and Linkage Design*, Balt, Indiana, pp. 2~3, 65~67.

Hartenberg, R. S. and Denavit, J., 1964, *Kinematic Synthesis of Linkages*, MacGraw-Hill, New York, pp. 59~63, pp. 295~306, 315~320.

Kim, H. R. and Newcombe, W. R., 1982, "The Effect of Cam Profile Errors and System Flexibility on Cam Mechanism Output," *Mechanism and Machine Theory*, Vol. 17, No. 1, pp. 57~71.

Norton, R. L., 1988, "Effect of Manufacturing Method on Dynamic Performance of Cams-an Experimental Study : Part I-Eccentric Cams and Part II-Double Dwell Cams," *Mechanism and Machine Theory*, Vol. 23, No. 3, pp. 191~208.

Norton, R. L., 2002, *Cam Design and Manufacturing Handbook*, Industrial, New York, pp. 315~334.

Pulkrabek, W. W., 1997, *Engineering Fundamentals of the Internal Combustion Engine*, Prentice-Hall, New Jersey, p. 16, 24.

Rao, S. S., 1984, "Error Analysis of Cam-Follower Systems : a Probablistic Approach," *Proceedings of the Institution of Mechanical Engineers-Part C, Journal of Mechanical Engineering Science*, Vol. 198, No. 12, pp. 155~162.

Rees-Jones, J., 1978, "Mechanisms, Cam Cutting Co-ordinates," *Engineering*, March, pp. 220~224.

Rees-Jones, J., 1978, "Mechanisms, Cam Curvature and Interference," *Engineering*, May, pp. 460~463.

Rothbart, H.A.(Ed.), 2004, *Cam Design Handbook*, McGraw-Hill, New York, pp. 285~301.

Spotts, M. F., 1985, *Design of Machine Elements*, 6th Edition, Prentice-Hall, New Jersey, p. 611.

Wang, W. H., Tseng, C. H., Tsay, C. B. and Ling, S. F., 1993, "On the Manufacturing Tolerance of Disk Cam Profile," *Journal of Materials Processing Technology*, Vol. 38, No. 1-2, pp. 71~84.

Wu, L. I., 2003, "Calculating Conjugate Cam Profiles by Vector Equations," *Proceedings of the Institution of Mechanical Engineers-Part C, Journal of Mechanical Engineering Science*, Vol. 217, No. 10, pp. 1117~1123.

Wu, L. I. and Chang, W. T., 2005, "Analysis of Mechanical Errors in Disk Cam Mechanisms," *Proceedings of the Institution of Mechanical Engineers-Part C, Journal of Mechanical Engineering Science*, Vol. 219, No. 2, pp. 209~224.